CONFERENCE PRE-PRINT

THE ROLE OF AMBIENT TURBULENCE IN FACILITATING THERMAL QUENCH OF DISRUPTIVE PLASMAS IN THE HL-2A TOKAMAK

Y. C. Li^1 , Y. Xu^1 , M. $Jiang^2$, J. $Cheng^1$, G. Z. Hao^2 , X. Q. $Wang^1$, Z. B. Shi^2 , Yi. Liu^2 , J. Q. Xu^2 , Y. P. $Zhang^2$, D. N. Wu^1 , J. $Huang^1$, W. Li^1 , H. $Zhou^1$ and J. R. $Shao^1$

E-mail contact of main author: liyucai@swjtu.edu.cn

Abstract

Plasma disruption in tokamaks is a serious challenge in fusion researches. While recent studies reveal that microturbulence may play a critical role in facilitating thermal quench (TQ) and ensuing disruption, experimental evidence linking turbulence to TQ dynamics is lacking. The present work reports the first direct experimental observation that turbulence makes significant contribution in accelerating TQ using high spatiotemporal resolution, two-dimensional image measurements. It is found that before TQ, during the initial heat transfer passing through the island X point, turbulence amplitudes and propagation characteristics abruptly increase, suggesting crucial impact on facilitating the TQ. The results provide important info for understanding intricate interaction between turbulence and macro-scale MHD instabilities, and hence, for efficiently controlling MHD instabilities and avoiding/mitigating disruption events in fusion devices.

1. INTRODUCTION

It is well-known that disruptions in tokamak plasmas are severe events which abruptly deteriorate plasma confinement. During thermal and current quenches, intense heat loads and substantial electromagnetic forces may damage divertors and other mechanical structures within the machine. In recent years, both experimental and theoretical studies have shown that plasma disruptions are generally associated with the uncontrolled growth of magnetohydrodynamic (MHD) instabilities [1-4]. Since large-scale MHD behaviors can be affected by plasma pressure and current profiles, both of which are influenced by small-scale turbulent transport [5-6], a complex interaction can occur between MHD instabilities and turbulence. Experimental studies [7-8] and numerical simulations [9-10] indicate that MHD instabilities can alter turbulence characteristics by modifying equilibrium profiles or local flow shear. Concurrently, the influence of plasma turbulence on MHDs has also been observed in various tokamaks [2, 11-14]. More recently, a study has unravelled the role of kinetic turbulence in changing MHD equilibrium through three-dimensional reconnection [15], further highlighting the significance of multi-scale interplay in affecting MHD behaviors. However, experimental evidence regarding the impact of ambient turbulence on the dynamic evolution of thermal quench (TQ) and subsequent disruptions remain scarce.

In the HL-2A tokamak, two sorts of disruptive discharges have been observed: one is characterized by a minor temperature drop preceding the TQ, whereas the other without such a precursor collapse [16]. Both types exhibit a common trend, namely, a significant enhancement of plasma turbulence before the TQ onset. This work presents an in-depth analysis of the dynamic evolutions of heat transport and background turbulence, along with their complex interplay during the TQ phase. The results show that prior to the TQ, when the initial heat flux ejects through the island's X-point, a remarkable increase takes place in the amplitude and spatial correlation in temperature fluctuations

¹ Institute of Fusion Science, School of Physical Science and Technology, Southwest Jiaotong University Chengdu 610031, China

² Southwestern Institute of Physics, Chengdu 610041, China

together with enhanced outward radial propagation. These changes are found to be linked to an increase of the local temperature gradient, which is caused by outward heat expulsion. The experimental results explicitly indicate that ambient turbulence may play a vital role in facilitating the TQ.

2. EXPERIMENTAL SETUP

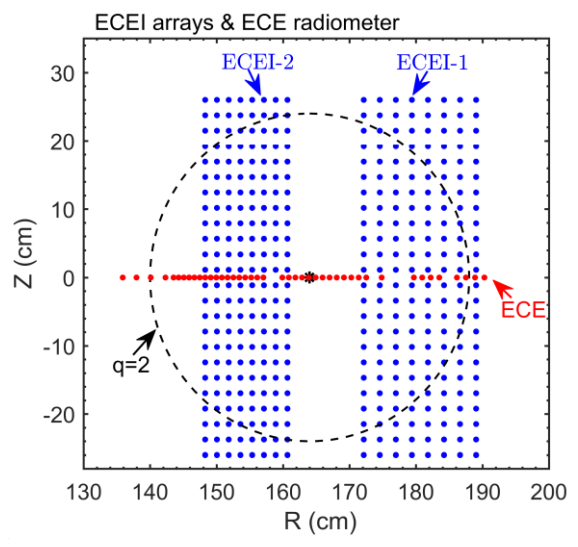


Figure 1 Measurement points of two ECEI arrays and the ECE radiometer. The black circle denotes the q=2 magnetic flux surface.

In this study, the experiment was carried out in the ohmically heated plasmas in the HL-2A tokamak with a limiter configuration. The major and minor radii are R = 164 cm and a ≈ 38 cm, respectively. The toroidal magnetic field $B_T = 1.32 \text{ T}$, plasma current $I_p \approx 136 \text{ kA}$, the central lineaveraged density $\bar{n}_{e0} \approx 0.9 \times 10^{19} \,\mathrm{m}^{-3}$, and the edge safety factorq(a) ≈ 4.3 . In this work the main diagnostics used are: two sets of 24 (vertical) × 8 (radial) electron cyclotron emission imaging (ECEI) arrays, which simultaneously measured the macro-scale electron temperature perturbation (δT_e) and micro-scale T_e fluctuations (\tilde{T}_e) with a sampling rate of 500 kHz and a spatial resolution of 1.8-2.3 cm [16–18]; a multi-channel ECE radiometer to measure the electron temperature (T_e) profile [19], and the absolute value of T_e was cross-calibrated with core channels of the Thomson scattering diagnostic [9]. The noise level of the ECE measurement is about 25%. The ECE and ECEI diagnostics were mounted at the same toroidal location of the torus and the spatial distributions of the 1D ECE (red color) and 2D ECEI (blue color) channels in the small cross-section are illustrated in Fig. 1. In this work, the q profile is calculated by the EFIT reconstruction [20], which is internally constrained by the Faraday rotation angle and externally constrained by the magnetic measurement. In Fig. 1, the q = 2 magnetic flux surface is denoted by the black circle, and hence, the view field of the images could capture the spatiotemporal evolution of most mode (or island) structures and their primary features within m/n < 2 surface. The magnetic fluctuations and mode numbers were detected by two sets of Mirnov coils surrounding the device wall with 18 distributed along the poloidal and 10 along the toroidal direction, respectively [21].

3. EXPERIMENTAL RESULTS AND DISCUSSIONS

Figure 2 shows typical temporal sequences of main discharge parameters across the TQ in a disruptive shot. Here, the onsets of the TQ and CQ take place at 823.5 ms and 824.1 ms, respectively. Nevertheless, the CQ phase is not the focus of this study. Note that in this study the start time of the TQ is defined by the drop in the core electron temperature (T_{e0}), although a fast heat transport event induces

a small T_e drop in the q=2 region before the core T_e reduction, as we elucidated earlier [17]. Before the TQ, the plasma density, soft X-ray and Mirnov signals all oscillate periodically, corresponding to rotation of the m/n=2/1 island, as illustrated by ECE images in Fig. 4. Prior to TQ, there is a sharp rise in the \dot{B}_{θ} signal (see blue curve in Fig. 2(d)), which reflects essentially the distortion of magnetic topology before the temperature collapse. The turbulence powers of magnetic fluctuations (\tilde{B}_{θ}^2 detected by Mirnov coil on the wall) and electron temperature fluctuations (\tilde{T}_e^2 detected by ECEI nearby the energy release spot) are plotted in Figs. 2(e) and (f), respectively. One can clearly see that both \tilde{B}_{θ}^2

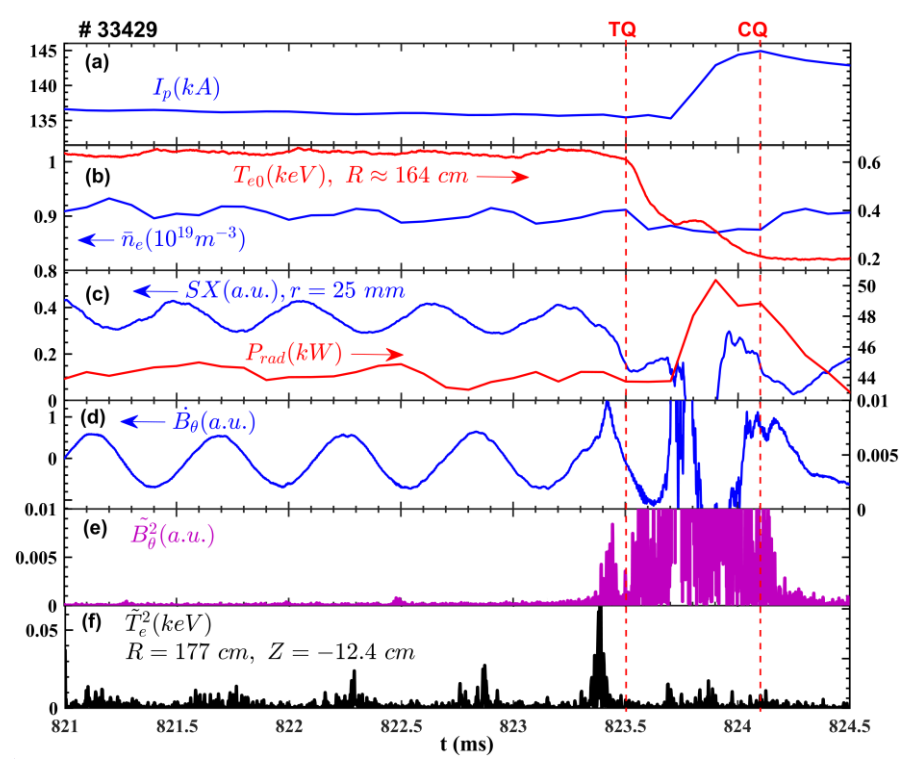


Figure 2 (a) Plasma current (I_p) ; (b) core electron temperature (T_{e0}) measured by the ECE and central line-averaged density (\bar{n}_e) ; (c) soft X-ray radiation (SX) and total radiated power (P_{rad}) ; (d) the magnetic oscillation (\dot{B}_θ) , (e)magnetic fluctuation power (\tilde{B}_θ^2) in the frequency range of 15–200 kHz measured by Mirnov coil and (f) electron temperature fluctuation power (\tilde{T}_e^2) in the frequency range of 15–100 kHz measured by ECEI.

and \tilde{T}_e^2 abruptly increase ahead of the TQ, and the electrostatic fluctuations burst at slightly different times from the magnetic fluctuations due to probably a time lag between the local T_e fluctuations and the magnetic fluctuations measured by pickup coils outside the plasma. In Fig. 2(f), the periodic fluctuations are modulated by the rotating island, i. e., a maximum at the X-point and a minimum at the O-point, consistent with gradient-driven turbulence. Analogous change has been observed in DIII-D and HL-2A [7, 9]. These results signify that both electrostatic and magnetic turbulence may play an essential role in facilitating the TQ. Similar phenomena of turbulence increase before plasma disruptions have also been reported in other tokamaks [2, 11-12].

MHD structure and dynamics before the disruption can be clearly detected by the 1D ECE radiometer and 2D ECE images by measuring the temperature profiles and perturbations with high temporal and spatial resolutions. To identify the detailed features of the modes prior to the TQ, in figure 3 we have plotted the radial dependences of T_e (measured at X- and O-points), the amplitude and phase of the T_e perturbation ($\delta T_e = T_e - \langle T_e \rangle$) detected by a horizontal multi-channel ECE radiometer. There co-exist an m/n = 2/1 tearing mode and an m/n = 1/1 mode. In the figure, the q=1 surface is roughly marked at $R \approx 151.6$ cm at the high-field side (HFS) and $R \approx 172$ cm at the low-field side (LFS),

for which the phase of δT_e on two sides of the axis ($R \approx 164$ cm) is reversed. The q=2 surface is roughly marked at $R \approx 140$ cm at the HFS and $R \approx 188$ cm at the LFS, and a π phase jump is clearly seen at the q=2 surface on both sides. Here, it is noticed that the q=1 surface is asymmetric around the axis, while the q=2 surface about the axis is nearly symmetric.

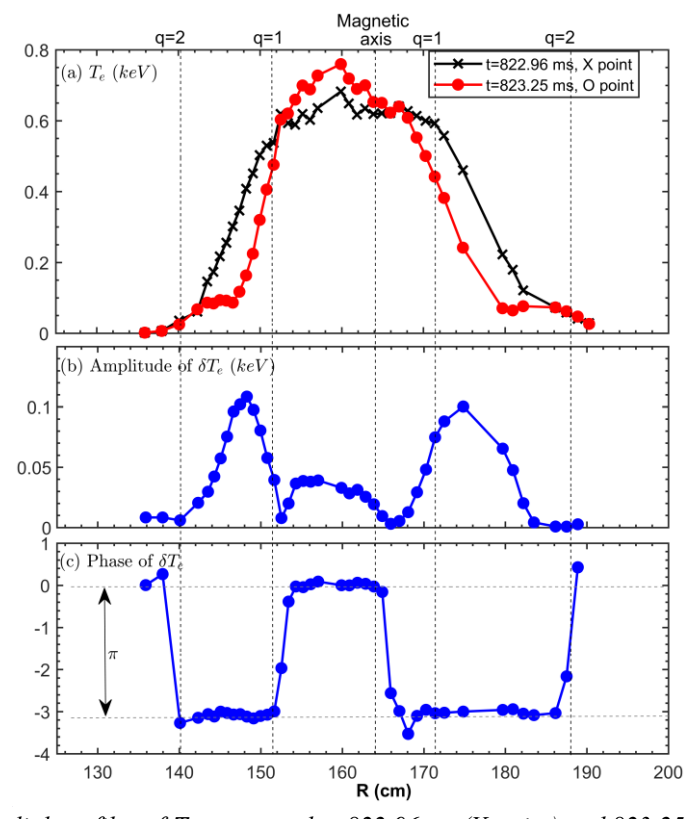


Figure 3 (a) radial profiles of T_e measured at 822.96 ms (X-point) and 823.25 ms (O-point), (b) radial profiles of amplitude of δT_e and (e) radial profiles of phase of δT_e .

In this investigation, we aim at exploring the detailed effects of ambient turbulence on the dynamic evolution of the energy quench, a critical process to result in plasma disruption. To do this, we have examined the characteristics of MHD instabilities and heat transport by analyzing temperature perturbations and heat flow patterns obtained from the 2D ECEI. This diagnostic technique enables simultaneous measurement of large-scale electron temperature perturbations δT_e and small-scale temperature fluctuations (\tilde{T}_e) [16]. Because the electron thermal velocity far exceeds the temporal resolution of ECEI imaging, it is reasonable to assume that transient heat flows depicted in $\delta T_e/\bar{T}_e$ contour plots align closely with local magnetic field lines, thereby reflecting modifications in magnetic topology [23]. Figure 4(a) displays the temporal evolution of $\delta T_e/\bar{T}_e$ (measured by ECEI at R=184.2 cm and Z=-3.4 cm) alongside the central electron temperature T_{e0} . The upper panels of Fig. 4(b) present a sequence of ECE images (labeled $1\rightarrow 3$) captured before the TQ, with the red circle indicating the q=2 magnetic flux surface. These images reveal that at the beginning the heat punctures through the island's X-point, followed by a substantial outward energy release, and meanwhile, a significant alteration in the magnetic topology via field line reconnection.

To survey the influence of turbulence on the heat transfer via the X-point, we have analysed the dynamic evolution of turbulence characters (e.g., propagation and correlation lengths) and their interplay with heat transfer in the above period. The radial propagation of electron temperature fluctuations (\tilde{T}_e in a frequency range of 15-100 kHz) along the heat transfer channel is evaluated by

calculating the coefficient of the cross-correlation function (CCF) of \tilde{T}_e detected in the ECEI pixel array ranged in $R \approx 172\text{-}187$ cm with a fixed Z = -12.4 cm (see the horizontal white line in ECEIs). Plotted in the middle graphs of Figs. 4(b) are the contour-plots of CCF (coefficient) as a function of time delay ($\Delta \tau$) around the time points $1 \rightarrow 3$. It shows that there exists a clear radially outward propagation in temperature fluctuations. The radial range of the turbulence outward propagation extends for about 10 cm with a phase velocity $\tilde{V}_{r,p} \approx 5$ km/s. To further assess the energy transfer of turbulence in the process, we also calculated the group velocity of \tilde{T}_e propagation by computing the CCF on the envelope of \tilde{T}_e signals. The result shows that the group velocity is about 1-3 km/s [24].

Here, a critical issue is to compare the timescale of heat transfer (T_e quench) with that of turbulence energy propagation. The onset of heat release through the magnetic island's X-point is governed by the magnetic reconnection time, $\tau_c \approx (\tau_R \cdot \tau_A)^{0.5}$, where $\tau_R = \mu_0 r^2/\eta$ represents the resistive diffusion time and $\tau_A = 2\pi q R_0/(B/\sqrt{\mu_0 m_i n})$ denotes the Alfvén transit time. Here, B, q, n, η , r and R_0 correspond to the local magnetic field strength, safety factor, plasma density, resistivity, minor radius, and major radius, respectively [23, 25]. Using experimental parameters B = 1.3 T, q = 2, $n = 0.9 \times 10^{19}$ m⁻³, $T_e = 0.09$ keV, $\eta = 1.03 \times 10^{-2} Z \cdot ln \Lambda \cdot T^{-1.5} \approx 1.7 \times 10^{-6} \Omega \cdot m$ (calculated via $\eta = 1.03 \times 10^{-2} Z \cdot ln \Lambda \cdot T^{-1.5} \approx 1.7 \times 10^{-6} \Omega \cdot m$), r = 20 cm, and $R_0 = 164$ cm, we obtain $\tau_c \approx 167 \mu s$, which is roughly an order of magnitude greater than the observed thermal quench timescale. In case

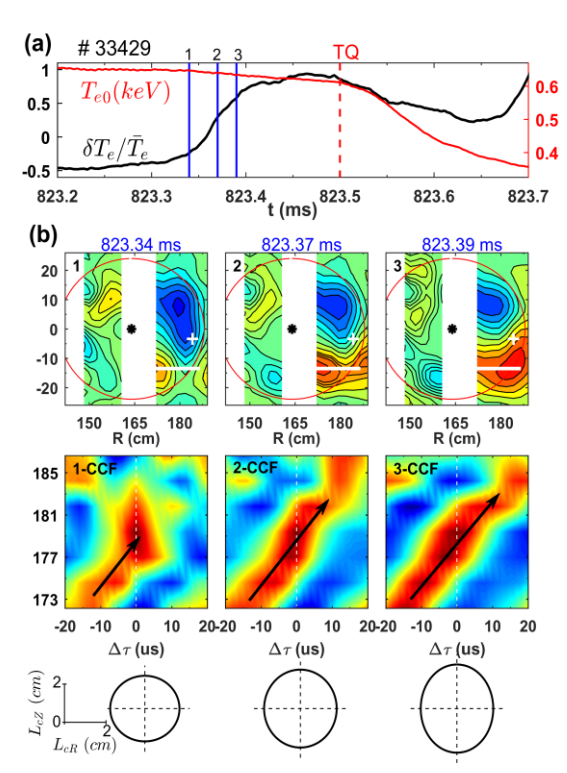


Figure 4 (a) Time evolutions of T_{e0} and $\delta T_e/T_e$ measured at R=184.2 cm and Z=-3.4 cm (see white cross in Fig. 2 (b)); (b) top: ECE images taken at 3 time points marked by blue vertical lines in (a), the 'asterisk' denotes the axis location, and the red circles are the q=2 flux surface; middle: contourplots of CCF of \tilde{T}_e as a function of time delay ($\Delta \tau$) at the above 3 time points ($1\rightarrow 3$); bottom: horizontal (L_{cR}) and vertical (L_{cZ}) correlation lengths of turbulence eddies.

that the resistive diffusion travels across a characteristic turbulence correlation length \sim 4 cm, the reconnection time can be reduced to around 30 μ s. This value remains comparable to or slightly longer than the turbulence energy propagation time. This result verifies that rapid turbulent transport may play a key role in accelerating heat expulsion and accelerating the subsequent thermal quench.

Furthermore, in Fig. 4(b) the CCF contour plots exhibit a notable size in spatial correlation of \tilde{T}_e during the heat transfer phase. For making a quantitative evaluation, the radial correlation length (L_{cR}) of \tilde{T}_e is derived from the e-folding distance of the CCF at zero time delay ($\Delta \tau = 0$). Similarly, the poloidal correlation length (L_{cZ}) is estimated by computing the poloidal CCF using \tilde{T}_e signals from an ECEI pixel array spanning Z = -3 cm to -17.5cm at a fixed radial position R = 179 cm (located nearby the X-point). The calculated L_{cR} and L_{cZ} are displayed in the bottom panels of Fig. 4(b) at time points approaching the TQ. Apparently, both correlation lengths increase significantly reaching up to ~4 cm, providing strong evidence for enhanced turbulence coherence and its contribution to promoting large-scale energy release prior to the thermal quench. These results are reproducible in several discharges with similar operational conditions. Notably, the observed correlation length (~4 cm) exceeds the typical size of individual

turbulence eddies (~1 cm), indicating the presence of avalanche-like transport mechanisms. This behavior may arise from self-similar structures within the turbulent plasma, as previously reported in refs [26-28].

In figure 4(b), the energy transfer across the X-point of the q=2 flux surface can be clearly observed. To further confirm it, in figure 5 we have plotted the time evolutions of ECEI signals both inside (ch# 56, 55, 54, 53) and outside (ch# 51, 50, 49) the q=2 surface along the heat transfer channel (see the horizontal white line in ECEIs in Fig. 4). One can see that before TQ, the temperature drops inside the q=2 surface and rises outside that surface, indicating an outward heat release via the q=2 surface.

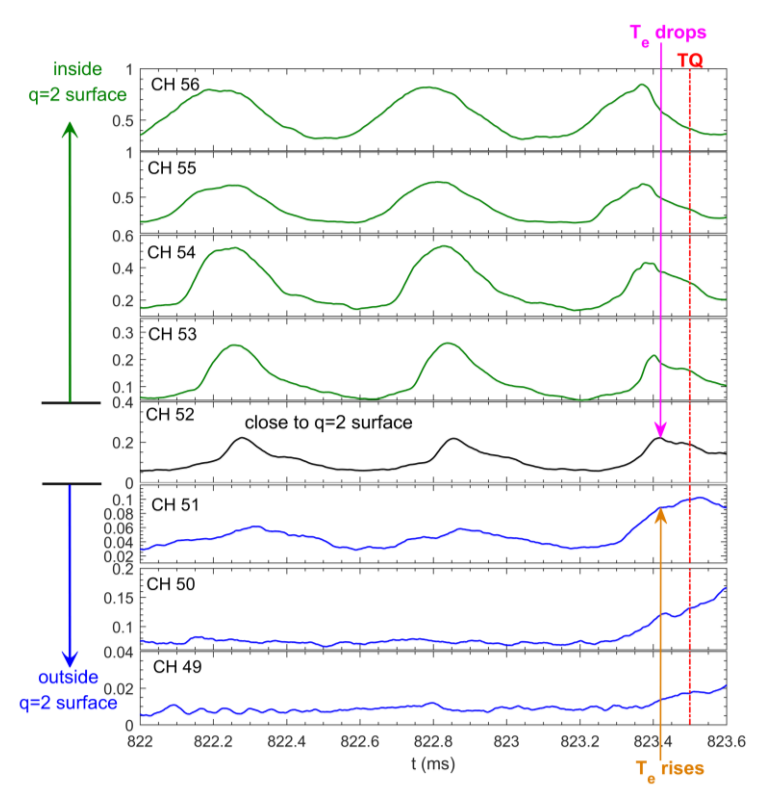


Figure 5 Time evolutions of ECEI signals inside and outside the q=2 surface along the heat transfer channel.

It is essential to investigate how turbulence characteristics evolve and interact with heat transport during the dynamic progression of the thermal quench (TQ). To address this, we have analyzed the temporal evolution of the equilibrium temperature gradient and its influence on the linear excitation of turbulence and associated turbulent transport near the location of heat transfer point. Figure 6(a) displays the time traces of electron temperature (T_e) measured by ECEI at various radial positions around the magnetic island's X-point, where $r = \sqrt{(R - R_0)^2 + (Z - Z_0)^2}$, with $R_0 = 164$ cm and $Z_0 = 0$. As previously reported [8, 29], T_e decreases when the O-point passes the measurement location and increases when the X-point approaches. At first glance, a gradual decline in the average T_e is observed as the TQ approaches, consistent with outward heat losses. A closer examination reveals that at the inner radial position (r = 9.91 cm), the blue curve shows nearly symmetric oscillations in T_e corresponding to alternating passages of the X- and O-points. In contrast, at outer locations, the duration of the O-point progressively longer than that of the X-point, indicating a gradual drop in local temperatures and consequently a modification of the T_e profile. For a comparison, the radially resolved T_e profiles, averaged over three specific time slices $(t_1, t_2$ and t_3) close to the X-point, are shown in Fig.

6(b). These profiles demonstrate an increasing steepness in the radial temperature gradient when the time approaches the TQ, particularly in the region $r \approx 12-20$ cm. Although the overall change in the T_e profile appears modest, theoretical models suggest that even slight enhancement in the temperature gradient can strongly influence turbulence excitation and the resulting intrinsic currents via ensemble averaging of turbulence coupling [5-6]. Indeed, experimental observations from the EAST tokamak have confirmed the generation of intrinsic currents driven by turbulence induced by T_e gradients [14]. More recent findings from DIII-D also unravel a correlation between increased T_e gradients and enhanced turbulence levels preceding sawtooth collapses [15]. The turbulence-induced currents inherently alter the local magnetic field structure, thus contributing to magnetic topology changes and reconnection before the TQ onset.

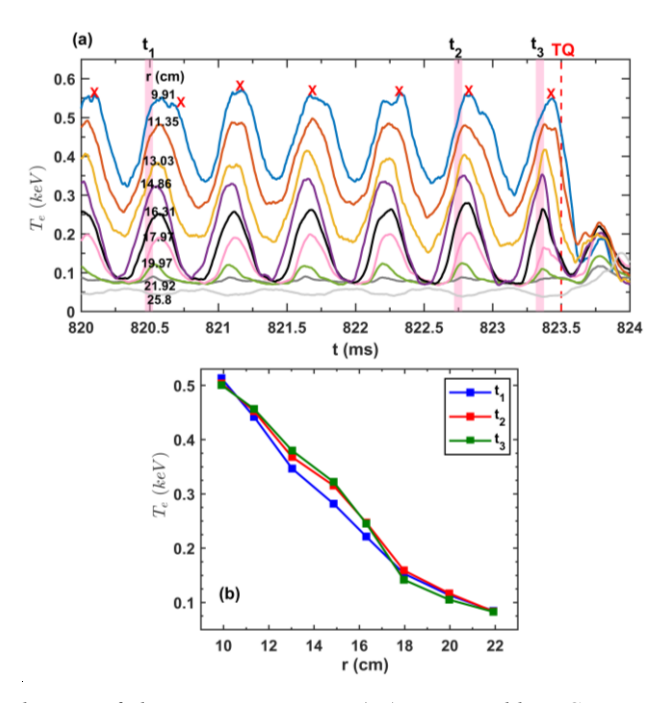


Figure. 6 (a) Time evolutions of electron temperature (T_e) measured by ECEI at various radial locations in the lower-right side nearby the heat transfer zone when approaching the TQ. Shown in (b) are comparisons of radial dependences of averaged T_e detected at three different time slices (t_1 , t_2 , t_3) nearby the X-point, as marked in (a).

The dynamic interplay between heat transport and ambient turbulence can be as follows: Due to certain triggering mechanisms, an initial heat leakage passes through the island's X-point, giving rise of temperature (or pressure) gradient in the surrounding region. This increased gradient acts as a driving source for turbulence, amplifying both turbulent fluctuations and associated transport processes. The intensified turbulence, in turn, induces local current perturbations and promotes magnetic reconnection, leading to the opening of magnetic field lines near the X-point. Consequently, plasma energy begins to escape radially outward, further sharpening the temperature (or pressure) gradient and increasing turbulent transport. This positive feedback loop drives the system into a self-sustaining regime, accelerating energy loss until the thermal quench is fully triggered.

4. SUMMARY

An extensive investigation has been conducted to delve into the dynamic evolution and intriguing interaction between plasma turbulence and heat transport during the thermal quench (TQ) preceding disruption in the HL-2A tokamak. Utilizing high spatiotemporal resolution two-dimensional electron cyclotron emission (ECE) imaging, we have obtained comprehensive information about MHD

instabilities, macroscopic electron temperature perturbations, heat flow patterns, and small-scale turbulent features. The results provide compelling evidence that ambient turbulence significantly contributes to the onset and progression of the TQ. During the initial stage of heat transfer through the magnetic island's X-point, a surge is observed in turbulence intensity, spatial correlation lengths, and propagation velocities, suggesting that ambient turbulence may play a vital role in facilitating the TQ. The interaction between turbulence and heat flux can be understood within a self-regulated regime: an initial heat leakage across the X-point steepens the local temperature (or pressure) gradient, which in turn amplifies turbulence and turbulent transport. This enhanced turbulence generates localized current perturbations and strengthens magnetic reconnection, leading to the opening of magnetic field lines near the X-point. As a result, additional plasma energy is rapidly expelled, further increasing the temperature gradient and intensifying turbulence. This feedback cycle continues to escalate, ultimately causing severe deformation of magnetic flux surfaces. The resulting large-scale energy release initiates the thermal quench and leads to plasma disruption. The results presented here offer new perspectives on multi-scale physical processes in magnetically confined plasmas, particularly highlighting how microscale turbulence can profoundly influence macro-scale MHD behavior and trigger disruptive events in tokamaks. Future experimental campaigns and advanced theoretical modeling are needed to pinpoint the critical thresholds and underlying mechanisms responsible for initiating the initial heat leakage through the X-point. These findings are beneficial for the control of MHD instabilities and avoidance of plasma disruptions in fusion devices.

REFERENCES

- [1] J. A. Wesson et al., Nucl. Fusion **29** (1989) 641.
- [2] G. Waidmann and G. L. Kuang, Nucl. Fusion 32 (1992) 645.
- [3] T. C. Hender et al., Nucl. Fusion 47 (2007) S128.
- [4] M. J. Choi et al., Nucl. Fusion **56** (2016) 066013.
- [5] F. L. Hinton, R. E. Waltz, and J. Candy, Phys. Plasmas 11, 2433 (2004).
- [6] W. X. Wang et al., Nucl. Fusion **59**, 084002 (2019).
- [7] L. Bardoczi et al., Phys. Rev. Lett. 116 (2016) 215001.
- [8] M. Jiang, Y. Xu et al., Nucl. Fusion **59** (2019) 066019.
- [9] D. Zarzoso et al., Nucl. Fusion 55 (2015) 113018.
- [10] T. S. Hahm et al., Phys. Plasmas 28 (2021) 022302.
- [11] A.Boileau et al., Nucl. Fusion 27 (1987) 109.
- [12] D. L. Brower, C. X. Yu et al., Phys. Rev. Lett. 67 (1991) 200.
- [13] M. J. Choi et al., Nat. Communications 12 (2021) 375.
- [14] E. Z. Li et al., Phys. Rev. Lett. 128 (2022) 085003.
- [15] G. Wang et al., Nucl. Fusion 64 (2024) 066024.
- [16] J. Y. Park et al., Nature 59 (2025) 644.
- [17] Y. C. Li et al., Sci. Rep. 13 (2023) 4785.
- [18] M. Jiang et al., Rev. Sci. Instrum. **84** (2013) 113501.
- [19] M. Jiang et al., Rev. Sci. Instrum. 86, (2015) 076107.
- [20] Z. B. Shi et al., Rev. Sci. Instrum. 85, (2014) 023510.
- [21] L. L. Lao, et al., Nucl. Fusion 30, 1035 (1990).
- [22] Q. W. Yang et al., Chin. Phys. Lett. 21 (2004) 2475.
- [23] H. K. Park et al., Phys. Rev. Lett. 96, (2006) 195003.
- [24] Y. C. Li et al., submitted to Phys. Rev. E (2025).
- [25] B. B. Kadomtsev, Sov. J. Plasma Phys 1 (1975) 389.
- [26] D. E. Newman et al., Phys. Plasmas 3 (1996) 1858.
- [27] P. A. Politzer, Phys. Rev. Lett. 84 (2000) 1192.
- [28] O. Pan, Y. Xu et al., Nucl. Fusion 55 (2015) 113010.
- [29] V. Igochine et al., Phys. Plasmas 21 (2014) 110702.